

Polarization tensor in spacetime of three dimensions and quantum field theoretical description of the nonequilibrium Casimir force in graphene systems

G. L. Klimchitskaya,^{1,2} C. C. Korikov,³ and V. M. Mostepanenko^{1,2}

¹*Central Astronomical Observatory at Pulkovo of the Russian Academy of Sciences, St.Petersburg, 196140, Russia*

²*Peter the Great Saint Petersburg Polytechnic University, Saint Petersburg, 195251, Russia*

³*Huawei Noah's Ark Lab, Krylatskaya str. 17, Moscow 121614, Russia*

The polarization tensor of graphene derived in the framework of the Dirac model using the methods of thermal quantum field theory in (2+1) dimensions is recast in a mathematically equivalent but more compact and convenient in computations form along the real frequency axis. The obtained unified expressions for the components of the polarization tensor are equally applicable in the regions of the on- and off-the-mass-shell electromagnetic waves. The advantages of the presented formalism are demonstrated on the example of nonequilibrium Casimir force in the configuration of two parallel graphene-coated dielectric plates one of which is either hotter or colder than the environment. This force is investigated as a function of temperature, the energy gap, and chemical potential of graphene coatings with account of the effects of spatial dispersion. Besides the thermodynamically nonequilibrium Casimir and Casimir-Polder forces, the obtained form of the polarization tensor can be useful for investigation of many diverse physical phenomena in graphene systems, such as surface plasmons, reflectances, electrical conductivity, radiation heat transfer, etc.

PACS numbers:

I. INTRODUCTION

An investigation of the physical properties of graphene, the two-dimensional sheet of carbon atoms, has inspired a renewed interest in the low-dimensional quantum field theory. The point is that at energies below approximately 3 eV graphene can be considered as a set of massless or very light quasiparticles described by the Dirac equation where the Fermi velocity v_F acts as the speed of light c [1–4]. This distinguishing feature converts graphene into a powerful tool accommodated on a laboratory table which can be used for testing such effects of fundamental physics as the Klein paradox [5], relativistic quantum Hall effect [6], creation from vacuum of the particle-antiparticle pairs in external fields [7–12] etc. Further still, a strong dependence of the dielectric properties of graphene on temperature gives no way of full understanding the reaction of graphene to the electromagnetic field without invoking the thermal quantum field theory in (2+1) dimensions.

The reaction of electrons or electronic quasiparticles to the electromagnetic field is described by the one-loop polarization tensor which has long been calculated in the frames of (2+1) dimensional quantum electrodynamics at zero temperature [13, 14] (see also Refs. [15–17]). Different aspects of the polarization tensor in application to graphene, including the case of nonzero temperature, were discussed in Refs. [18–21].

The reflection coefficients on a graphene sheet at zero temperature were expressed [22] via the polarization tensor of Refs. [13, 14]. The values of these reflection coefficients along the imaginary frequency axis were used for calculation of the equilibrium zero-temperature Casimir force in graphene systems [22]. In order to investigate this force at nonzero temperature, the polarization tensor of graphene was found at the pure imaginary Matsubara frequencies taking into account the nonzero energy gap (mass of quasiparticles) and the possible presence of doping (i.e., some foreign atoms) described

by the chemical potential [23]. Next, the polarization tensor of gapped graphene was analytically continued to the entire plane of complex frequencies including the real frequency axis [24]. A generalization of these results for the case of doped graphene was provided in Ref. [25]. In Ref. [26], it was shown that the obtained tensor is unique and cannot be further modified with no violation of the fundamental physical principles.

The expressions for the polarization tensor valid at the pure imaginary Matsubara frequencies obtained in Ref. [23] made it possible to calculate the thermal Casimir and Casimir-Polder interactions in many graphene systems [27–33]. As to the expressions for this tensor derived in Ref. [24], which are applicable over the entire plane of complex frequencies, they are of multi-purpose character and were used not only for calculation of the thermal Casimir and Casimir-Polder forces [34–42] but also for investigation of the reflectivity properties [43–45], electrical conductivity [46–49], and the surface plasmons [50–52] for graphene.

The Casimir force is the physical phenomenon determined by the electromagnetic fluctuations which occurs in the state of thermal equilibrium when temperatures of two interacting parallel plates are equal to each other and also equal to the temperature of the environment. In this case, the Casimir force is described by the Lifshitz theory [53–55]. The condition of thermal equilibrium may be, however, violated. This happens, for instance, when the temperature of at least one plate is not equal to that of the environment.

As long as the local thermal equilibrium holds, the Lifshitz theory was generalized to the situations when the standard (global) condition of thermal equilibrium is violated. The resulting theory allowed calculation of the nonequilibrium Casimir force between two parallel plates [56–60] and the Casimir-Polder force between a small particle and a dielectric plate [61, 62]. These calculations demand a knowledge of the reflection coefficients at both the Matsubara frequencies and along the real frequency axis. In the course of

further work, the developed theory was adapted for calculation of the nonequilibrium Casimir and Casimir-Polder forces between the arbitrarily shaped bodies [63–70]. In all these cases, however, it was assumed that the dielectric response of all involved materials is temperature-independent.

In Ref. [71], the theory of the nonequilibrium Casimir force was generalized to situations where the dielectric permittivities of interacting bodies may depend on temperature. The developed formalism was applied [71] to the nonequilibrium Casimir force between two metallic plates kept at different temperatures taking into account the dependence of the relaxation parameter on temperature. Using the same formalism, the nonequilibrium Casimir-Polder force was considered between different atoms and a plate made of the material which undergoes the phase transition with increasing temperature [72].

As was noted above, the dielectric properties of graphene described by the polarization tensor strongly depend on temperature. Because of this, it is likely that the nonequilibrium Casimir effect in graphene systems has considerable opportunities for both theoretical and experimental investigation. Until the present time, few investigations have been conducted of the nonequilibrium Casimir-Polder force between nanoparticles and the freestanding sheets of both the pristine [73] and gapped [74] graphene. The cases when nanoparticles interact with either heated or cooled plates coated with gapped [75] or both gapped and doped [76] graphene were also considered using the formalism of the polarization tensor. However, the most interesting case of the nonequilibrium Casimir force between two plates coated with graphene sheets was considered only in a single paper using the Kubo formalism [77], where the energy gap was put equal to zero and the spatial dispersion in the dielectric response of graphene was neglected.

In this paper, we obtain the more convenient analytic form for the polarization tensor of graphene along the real frequency axis. Unlike the previously used forms, which express the components of the polarization tensor in the regions of the on-the-mass-shell and off-the-mass-shell electromagnetic waves using different functions, here we present the more unified expressions for various relationships between the frequency and the wave vector. These expressions are mathematically equivalent to that ones of Refs. [24, 26, 42, 76] but are more convenient for calculation of the physical quantities expressed via the polarization tensor defined along the real frequency axis.

To illustrate the advantages of the suggested form of the polarization tensor, we investigate the nonequilibrium Casimir force in the configuration of two parallel plates coated with real graphene sheets characterized by the nonzero energy gap and chemical potential. The computations are made taking into account the effects of spatial dispersion in the dielectric response of graphene coating described by means of the polarization tensor. In the configuration considered, the temperature of one graphene-coated plate is the same as of the environment and of another one can be either higher or lower than that of the environment.

According to our results, the presence of graphene coatings increases the magnitudes of both equilibrium and nonequilibrium

Casimir pressures. The dependence of this increase on the energy gap and chemical potential of graphene coatings is investigated. It is shown that the magnitude of the nonequilibrium Casimir pressure on a cooled graphene-coated plate is less than that of the equilibrium pressure, whereas the magnitude of the nonequilibrium pressure on a heated plate is larger than that of the equilibrium one. For a cooled plate, the effects of nonequilibrium are larger for a smaller energy gap, but for a heated plate they are larger for a larger energy gap. An impact of the energy gap decreases with increasing chemical potential. The relative error in the nonequilibrium Casimir pressure arising due to neglect of the spatial dispersion in the dielectric response of graphene coating is found as the function of plate temperature, the energy gap, and chemical potential of graphene coatings. It increases with increasing energy gap and, for a cooled plate coated with graphene characterized by the zero chemical potential, may reach 50% for the temperature of 77 K. For a heated up to 500 K graphene-coated plate, the relative error due to a neglect of the spatial dispersion is shown to be below 9%.

The paper is organized as follows. In Sec. II, we present the suggested form of the polarization tensor of graphene defined along the real frequency axis. The previously obtained expressions at the pure imaginary Matsubara frequencies also required in computations remain unchanged. Section III contains the brief list of expressions for the nonequilibrium Casimir pressure between two graphene-coated dielectric plates. In Sec. IV, the computational results are presented for the nonequilibrium Casimir pressure in the configuration of two silica glass plates coated with graphene sheets characterized by different values of the energy gap and chemical potential. These results take full account of the spatial dispersion in graphene coatings. Section V contains our conclusions and a discussion of the obtained results.

Below we do not put to unity the fundamental constants \hbar and c in order to simplify an employment of the obtained results in various future applications.

II. POLARIZATION TENSOR OF GRAPHENE ALONG THE REAL FREQUENCY AXIS

We start from the expressions for the polarization tensor of graphene $\Pi_{\beta\gamma}(\omega, k, T)$ obtained in Refs. [24–26] where $\beta, \gamma = 0, 1, 2$, ω is the frequency, k is the magnitude of the wave vector projection on the plane of graphene, and T is the temperature of a graphene sheet. The components of the polarization tensor also depend on the energy gap Δ and chemical potential μ which are not indicated explicitly for the sake of brevity.

It is convenient to express the reflection coefficients on a graphene sheet and other quantities of physical significance via the component $\Pi_{00}(\omega, k, T)$ and the following combination of the components of the polarization tensor

$$\Pi(\omega, k, T) \equiv k^2 \Pi_{\beta}^{\beta}(\omega, k, T) + \left(\frac{\omega^2}{c^2} - k^2 \right) \Pi_{00}(\omega, k, T). \quad (1)$$

The quantities Π_{00} and Π are conveniently presented as the

sums of two contributions

$$\begin{aligned}\Pi_{00}(\omega, k, T) &= \Pi_{00}^{(0)}(\omega, k) + \Pi_{00}^{(1)}(\omega, k, T), \\ \Pi(\omega, k, T) &= \Pi^{(0)}(\omega, k) + \Pi^{(1)}(\omega, k, T),\end{aligned}\quad (2)$$

where $\Pi_{00}^{(0)}$ and $\Pi^{(0)}$ are calculated at $T = 0$, $\mu = 0$. These contributions are in fact obtained by calculating the one-loop diagram within the standard quantum field theory at zero temperature [13, 14, 26]. As to the full quantities Π_{00} and Π , they are found by calculating the same diagram using the thermal quantum field theory in the Matsubara formulation with subsequent analytic continuation of the obtained results to the real frequency axis [24, 26].

We begin with the contributions $\Pi_{00}^{(0)}$ and $\Pi^{(0)}$ to Eq. (2). In some previous literature (see, e.g., Refs. [24, 26, 42, 76]) these contributions were expressed differently in the regions of the off-the-mass-shell waves satisfying the condition $\omega < v_F k$ (the strongly evanescent waves) and $\omega \geq v_F k$ (the off-the-mass-shell plasmonic waves with $v_F k \leq \omega < ck$ and the on-the-mass-shell propagating waves with $\omega \geq ck$). Here we present the following mathematically equivalent unified expressions which are valid over the entire axis of real frequencies:

$$\begin{aligned}\Pi_{00}^{(0)}(\omega, k) &= \frac{2\alpha\hbar ck^2}{\sqrt{v_F^2 k^2 - \omega^2}} \Psi\left(\frac{\Delta}{\hbar\sqrt{v_F^2 k^2 - \omega^2}}\right), \\ \Pi^{(0)}(\omega, k) &= \frac{2\alpha\hbar k^2}{c} \sqrt{v_F^2 k^2 - \omega^2} \Psi\left(\frac{\Delta}{\hbar\sqrt{v_F^2 k^2 - \omega^2}}\right),\end{aligned}\quad (3)$$

where $\alpha = e^2/(\hbar c)$ is the fine structure constant and the function Ψ is defined as

$$\Psi(x) = x + (1 - x^2) \arctan\left(\frac{1}{x}\right).\quad (4)$$

When using Eq. (3) in different frequency regions, the branch of the square root should be chosen as [24]

$$\sqrt{\omega^2 - v_F^2 k^2} = i\sqrt{v_F^2 k^2 - \omega^2}.\quad (5)$$

This rule assures that the spatially nonlocal dielectric permittivities of graphene defined via the polarization tensor have the positive imaginary parts. Note that in the frequency region $\omega < v_F k$ the quantities (3) are real. However, if $\omega \geq v_F k$, the quantities (3) are real if the condition $\Delta > \hbar\sqrt{\omega^2 - v_F^2 k^2}$ is satisfied and are complex under the opposite inequality $\Delta \leq \hbar\sqrt{\omega^2 - v_F^2 k^2}$. The transition from real to complex values of the quantities (3) corresponds to crossing the threshold of pair creation.

Now we consider the contributions $\Pi_{00}^{(1)}$ and $\Pi^{(1)}$ to Eq. (2). The first of them can be conveniently expressed via the following function:

$$X_1(x) = \frac{x^2 - v_F^2 k^2}{\sqrt{(\omega^2 - v_F^2 k^2)[x^2 - v_F^2 k^2 A(\omega, k)]}},\quad (6)$$

where

$$A(\omega, k) = 1 - \frac{\Delta^2}{\hbar^2(\omega^2 - v_F^2 k^2)}.\quad (7)$$

Using these notations, the quantity $\Pi_{00}^{(1)}$ in the entire region $\omega < v_F k$ and in the region $\omega \geq v_F k$ under the condition $\hbar\sqrt{\omega^2 - v_F^2 k^2} < \Delta$ is given by

$$\Pi_{00}^{(1)}(\omega, k, T) = \frac{4\alpha\hbar c}{v_F^2} \int_{\Delta/\hbar}^{\infty} dv w(v, \mu, T) \left[1 - \frac{1}{2} \sum_{\lambda=\pm 1} \lambda X_1(v + \lambda\omega) \right],\quad (8)$$

where

$$w(v, \mu, T) = \left[\exp\left(\frac{\hbar v + 2\mu}{2k_B T}\right) + 1 \right]^{-1} + \left[\exp\left(\frac{\hbar v - 2\mu}{2k_B T}\right) + 1 \right]^{-1}.\quad (9)$$

In the remaining region $\omega \geq v_F k$ under the opposite condition $\hbar\sqrt{\omega^2 - v_F^2 k^2} \geq \Delta$ the result is

$$\begin{aligned}\Pi_{00}^{(1)}(\omega, k, T) &= \frac{4\alpha\hbar c}{v_F^2} \left\{ \int_{\Delta/\hbar}^{v_0} dv w(v, \mu, T) \left[1 - \frac{1}{2} \sum_{\lambda=\pm 1} X_1(v + \lambda\omega) \right] \right. \\ &\quad \left. + \int_{v_0}^{\infty} dv w(v, \mu, T) \left[1 - \frac{1}{2} \sum_{\lambda=\pm 1} \lambda X_1(v + \lambda\omega) \right] \right\},\end{aligned}\quad (10)$$

where $v_0 = \omega - v_F k$. Note that the quantity (8) considered in the region $\omega \geq v_F k$, $\hbar\sqrt{\omega^2 - v_F^2 k^2} < \Delta$ is real. It is, however, complex in the entire region $\omega < v_F k$. The quantity (10) is complex as well.

The contribution $\Pi^{(1)}$ to Eq. (2) is conveniently expressed via the function

$$X_2(x) = \frac{\hbar^2(\omega^2 - v_F^2 k^2)x^2 + v_F^2 k^2 \Delta^2}{\hbar^2 \sqrt{(\omega^2 - v_F^2 k^2)[x^2 - v_F^2 k^2 A(\omega, k)]}}.\quad (11)$$

As a result, in the entire region $\omega < v_F k$ and in the region $\omega \geq v_F k$ under the condition $\hbar\sqrt{\omega^2 - v_F^2 k^2} < \Delta$, one obtains

$$\begin{aligned}\Pi^{(1)}(\omega, k, T) &= \frac{4\alpha\hbar\omega^2}{cv_F^2} \int_{\Delta/\hbar}^{\infty} dv w(v, \mu, T) \\ &\quad \times \left[1 - \frac{1}{2\omega^2} \sum_{\lambda=\pm 1} \lambda X_2(v + \lambda\omega) \right].\end{aligned}\quad (12)$$

This expression is real for $\omega \geq v_F k$, $\hbar\sqrt{\omega^2 - v_F^2 k^2} < \Delta$ and complex for $\omega < v_F k$.

In the remaining region $\omega \geq v_F k$, $\hbar\sqrt{\omega^2 - v_F^2 k^2} \geq \Delta$, the result is complex

$$\begin{aligned}\Pi^{(1)}(\omega, k, T) &= \frac{4\alpha\hbar\omega^2}{cv_F^2} \left\{ \int_{\Delta/\hbar}^{v_0} dv w(v, \mu, T) \right. \\ &\quad \times \left[1 - \frac{1}{2\omega^2} \sum_{\lambda=\pm 1} X_2(v + \lambda\omega) \right] \\ &\quad \left. + \int_{v_0}^{\infty} dv w(v, \mu, T) \left[1 - \frac{1}{2\omega^2} \sum_{\lambda=\pm 1} \lambda X_2(v + \lambda\omega) \right] \right\}.\end{aligned}\quad (13)$$

Equations (8), (10), (12), and (13) are mathematically equivalent to the corresponding expressions for $\Pi_{00}^{(1)}$ and $\Pi^{(1)}$ in Refs. [24, 26, 42, 76] where they are written in a more complicated form.

III. NONEQUILIBRIUM CASIMIR PRESSURE IN THE CONFIGURATION OF TWO GRAPHENE-COATED PLATES

We consider the configuration of two parallel dielectric plates spaced at the separation a made of a material with the frequency-dependent dielectric permittivity ε coated by the sheets of graphene characterized by the energy gap Δ and chemical potential μ . Let the first graphene-coated plate have the same temperature as the environment, $T_1 = T_E$. The temperature of the second graphene-coated plate, T_2 , can be either lower or higher than the environmental temperature T_E .

In this configuration, the nonequilibrium Casimir pressure on the second plate can be presented as the sum of two contributions [59, 60, 71]

$$P_{\text{neq}}(a, T_1, T_2) = P_{\text{qeq}}(a, T_1, T_2) + \Delta P_{\text{neq}}(a, T_1, T_2), \quad (14)$$

where P_{qeq} can be called the quasi equilibrium contribution

and ΔP_{neq} — the proper nonequilibrium contribution.

A few words about the assumptions used in derivation of Eq. (14) are in order. It has been known that the standard Lifshitz formula describing the equilibrium Casimir force was originally derived [53–55] using the correlations of the polarization field expressed via the fluctuation-dissipation theorem. These correlations are spatially local. Then, it is reasonable to admit that in the nonequilibrium situation, where the temperatures of two plates are different, the sources correlations are given by the same equations of the fluctuation-dissipation theorem with the appropriate temperatures [59]. This is a condition of the local thermal equilibrium employed in the derivation of an expression for the nonequilibrium Casimir force. Using this condition, the correlations of the electromagnetic field in the gap between the plates can be represented as the sum of correlations produced by the fluctuating polarizations in the materials of the first and second plates with the dielectric functions ε_1 and ε_2 kept at the temperatures T_1 and T_2 , respectively [59]. The condition of the local thermal equilibrium was also used in the classical paper [78] on the theory of radiative heat transfer.

We begin with the proper nonequilibrium contribution which can be presented in the form [59, 60, 71]

$$\Delta P_{\text{neq}} = \frac{\hbar c}{64\pi^2 a^4} \int_0^\infty u^3 du [n(u, T_1) - n(u, T_2)] \sum_\kappa \left[\int_0^1 t \sqrt{1-t^2} dt \frac{|R_\kappa(u, t, T_2)|^2 - |R_\kappa(u, t, T_1)|^2}{|D_\kappa(u, t, T_1, T_2)|^2} - 2 \int_1^\infty t \sqrt{t^2-1} e^{-u\sqrt{t^2-1}} dt \frac{\text{Im}R_\kappa(u, t, T_1)\text{Re}R_\kappa(u, t, T_2) - \text{Re}R_\kappa(u, t, T_1)\text{Im}R_\kappa(u, t, T_2)}{|D_\kappa(u, t, T_1, T_2)|^2} \right]. \quad (15)$$

Here,

$$D_\kappa(u, t, T_1, T_2) = 1 - R_\kappa(u, t, T_1)R_\kappa(u, t, T_2) e^{iu\sqrt{1-t^2}},$$

$$n(u, T_j) = \left(\exp \frac{\hbar c u}{2ak_B T_j} - 1 \right)^{-1}, \quad j = 1, 2, \quad (16)$$

and the dimensionless integration variables $u = 2a\omega/c$ and

$t = ck/\omega$ are expressed via the frequency and the wave vector projection.

The reflection coefficients on the graphene-coated plates for the transverse magnetic ($\kappa = \text{TM}$) and transverse electric ($\kappa = \text{TE}$) polarizations of the electromagnetic field are given by [79]

$$R_{\text{TM}}(\omega, k, T_{1,2}) = \frac{\hbar k^2 [\varepsilon(\omega)q(\omega, k) - \tilde{q}(\omega, k)] + q(\omega, k)\tilde{q}(\omega, k)\Pi_{00}(\omega, k, T_{1,2})}{\hbar k^2 [\varepsilon(\omega)q(\omega, k) + \tilde{q}(\omega, k)] + q(\omega, k)\tilde{q}(\omega, k)\Pi_{00}(\omega, k, T_{1,2})},$$

$$R_{\text{TE}}(\omega, k, T_{1,2}) = \frac{\hbar k^2 [q(\omega, k) - \tilde{q}(\omega, k)] - \Pi(\omega, k, T_{1,2})}{\hbar k^2 [q(\omega, k) + \tilde{q}(\omega, k)] + \Pi(\omega, k, T_{1,2})}. \quad (17)$$

In these equations, $q(\omega, k) \equiv \sqrt{k^2 - \omega^2/c^2}$, $\tilde{q}(\omega, k) \equiv \sqrt{k^2 - \varepsilon(\omega)\omega^2/c^2}$, and the polarization tensor is defined in Eqs. (2), (3), (8), (10), (12), and (13). The expressions for

the reflection coefficients (17) in terms of the dimensionless variables u and t are obtained by substituting $\omega = cu/(2a)$ and $k = tu/(2a)$ in Eq. (17). The result is

$$\begin{aligned}
R_{\text{TM}}(u, t, T_{1,2}) &= \frac{\hbar t^2 u [\varepsilon(u) \sqrt{t^2 - 1} - \sqrt{t^2 - \varepsilon(u)}] + 2a \sqrt{t^2 - 1} \sqrt{t^2 - \varepsilon(u)} \Pi_{00}(u, t, T_{1,2})}{\hbar t^2 u [\varepsilon(u) \sqrt{t^2 - 1} + \sqrt{t^2 - \varepsilon(u)}] + 2a \sqrt{t^2 - 1} \sqrt{t^2 - \varepsilon(u)} \Pi_{00}(u, t, T_{1,2})}, \\
R_{\text{TE}}(u, t, T_{1,2}) &= \frac{\hbar t^2 u^3 [\sqrt{t^2 - 1} - \sqrt{t^2 - \varepsilon(u)}] - 8a^3 \Pi(u, t, T_{1,2})}{\hbar t^2 u^3 [\sqrt{t^2 - 1} + \sqrt{t^2 - \varepsilon(u)}] + 8a^3 \Pi(u, t, T_{1,2})}.
\end{aligned} \tag{18}$$

We continue with the quasi-equilibrium contribution P_{qeq} to the nonequilibrium Casimir pressure (14). This name reflects the fact that it is calculated by the combination of the

Lifshitz-type formulas written along the imaginary frequency axis with appropriately taken into account temperatures of the graphene-coated plates

$$\begin{aligned}
P_{\text{qeq}}(a, T_1, T_2) &= -\frac{k_B}{2\pi} \left[T_1 \sum_{l=0}' \int_0^\infty q_{l,1} k dk \sum_k \frac{R_\kappa(i\xi_{l,1}, k, T_1) R_\kappa(i\xi_{l,1}, k, T_2)}{e^{2q_{l,1}a} - R_\kappa(i\xi_{l,1}, k, T_1) R_\kappa(i\xi_{l,1}, k, T_2)} \right. \\
&\quad \left. + T_2 \sum_{l=0}' \int_0^\infty q_{l,2} k dk \sum_k \frac{R_\kappa(i\xi_{l,2}, k, T_1) R_\kappa(i\xi_{l,2}, k, T_2)}{e^{2q_{l,2}a} - R_\kappa(i\xi_{l,2}, k, T_1) R_\kappa(i\xi_{l,2}, k, T_2)} \right].
\end{aligned} \tag{19}$$

Here, k_B is the Boltzmann constant, $\xi_{l,1(2)} = 2\pi k_B T_{1(2)} l / \hbar$ with $l = 0, 1, 2, \dots$ are the Matsubara frequencies calculated either at temperature T_1 or T_2 , the reflection coefficients R_κ are obtained from Eq. (17) by putting $\omega = i\xi_{l,1(2)}$, $q_{l,1(2)} \equiv q(i\xi_{l,1(2)}, k)$, and the prime on the sums in l divides the term with $l = 0$ by 2.

The expressions for the polarization tensor at the pure imaginary frequencies $\omega = i\xi_{l,1(2)}$ entering the reflection coefficients (17) are obtained from Eq. (3) and Eqs. (8), (12) valid for the region $\omega < v_F k$ with an appropriate choice of the branch of square roots. We do not present them here because they are contained in many papers (see, e.g., Refs. [36, 37, 39, 76]).

The term quasi equilibrium regarding the quantity (19) is also justified by the fact that for the temperature-independent dielectric response of the plate materials (this is the case, for instance, for the silica glass plates in the absence of graphene coating) the reflection coefficients in Eq. (19) depend on the temperature only implicitly through the Matsubara frequencies. In this case the proper nonequilibrium contribution (15) vanishes and the quasi equilibrium contribution (19) is expressed as a half of a sum of the truly equilibrium Casimir pressures calculated at the temperatures of the plates [56]. As a result,

$$P_{\text{neq}}(a, T_1, T_2) = P_{\text{qeq}}(a, T_1, T_2) = \frac{1}{2} [P_{\text{eq}}(a, T_1) + P_{\text{eq}}(a, T_2)]. \tag{20}$$

Each term in this equation is calculated by the standard Lifshitz formula under an assumption that the environmental temperature is the same as of the plate, i.e., T_1 for the first plate and T_2 for the second plate.

IV. APPLICATION TO NONEQUILIBRIUM CASIMIR PRESSURE IN CONFIGURATION OF TWO DIELECTRIC PLATES COATED WITH REAL GRAPHENE SHEETS

As an example of the presented formalism, we consider two parallel silica glass plates coated with real graphene sheets. The presence of a substrate along with the influence of foreign atoms and electron-electron interactions give rise to some nonzero energy gap Δ in the spectrum of graphene quasiparticles [20, 80, 81]. As to the foreign atoms, they result in a nonzero value of the chemical potential μ of graphene coating. The polarization tensor of graphene considered above takes into account both these parameters. A dependence of the polarization tensor on the magnitude of wave vector projection k reflects the effects of spatial dispersion in the dielectric response of graphene.

Computations of the Casimir pressure on the second plate are made for the cases when it is either heated up to $T_2 = 500$ K or cooled down to $T_2 = 77$ K. In so doing the temperature of the first plate is kept the same as that of the environment $T_1 = T_E = 300$ K. The proper nonequilibrium contribution ΔP_{neq} to the Casimir pressure P_{neq} was computed by Eqs. (15) and (18) where the polarization tensor of graphene coating is given by Eqs. (2), (3), (8), (10), (12), and (13). The dielectric permittivity of the plate along the real frequency axis was obtained from the tabulated optical data of silica glass [82] (see Ref. [83] for more details). The quasi equilibrium contribution P_{qeq} to the Casimir pressure P_{neq} was computed by Eqs. (19) and (17). The dielectric permittivity of silica glass at the pure imaginary Matsubara frequency axis was obtained from $\text{Im} \varepsilon(\omega)$ by using the Kramers-Kronig relation [83].

Below the computational results for the nonequilibrium

Casimir pressure are compared with those for the equilibrium one at $T_E = 300$ K. The latter are computed by Eqs. (19) and (20) with $T_1 = T_2 = T_E = 300$ K. To investigate the role of graphene coating, the obtained results for the case of graphene-coated plates are compared with the case of uncoated SiO_2 plates. For this purpose, one should put $\Pi_{00} = \Pi = 0$ in the reflection coefficients (17) and (18). Finally, we investigate the effect of spatial dispersion in the dielectric response of graphene coating on the Casimir pressure. To obtain the Casimir pressure in the spatially local approximation, i.e., with the effects of spatial dispersion disregarded, we use expressions (2), (3), (8), (10), (12), and (13) for the polarization tensor in the limiting case $v_F k/\omega \rightarrow 0$.

In Fig. 1, the role of the effects of nonequilibrium is illustrated for the uncoated SiO_2 plates. For this purpose, the ratios of nonequilibrium pressures $P_{\text{neq}}^{\text{SiO}_2}$ at the temperatures of the second plate $T_2 = 500$ K and 77 K to the classical limit of the equilibrium pressure at $T_E = 300$ K, $P_{\text{cl}}^{\text{SiO}_2}$, are shown by the top and bottom lines, respectively, as the functions of separation between the plates. Here, the classical limit of the

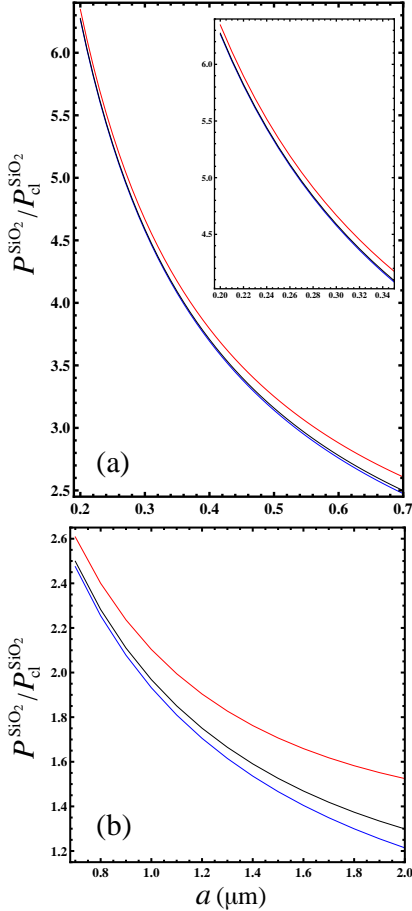


FIG. 1: The ratios of the nonequilibrium Casimir pressures for the uncoated SiO_2 plates (top and bottom lines for the plate temperatures of 500 K and 77 K, respectively) and of the equilibrium pressure (the middle line) to the classical limit of the equilibrium pressure are shown as the functions of separation in the distance ranges (a) from 0.2 to 0.7 μm and from 0.2 to 0.35 μm in the inset on an enlarged scale and (b) from 0.7 to 2 μm .

equilibrium Casimir pressure is given by [83]

$$P_{\text{cl}}^{\text{SiO}_2}(a, T) = -\frac{k_B T}{8\pi a^3} \text{Li}_3 \left[\left(\frac{\epsilon_0 - 1}{\epsilon_0 + 1} \right)^2 \right], \quad (21)$$

where $\text{Li}_3(z)$ is the polylogarithm function and the static dielectric permittivity of silica glass is $\epsilon_0 = 3.81$.

The middle lines in Fig. 1 show the dependence on separation for the equilibrium Casimir pressure $P_{\text{eq}}^{\text{SiO}_2}/P_{\text{cl}}^{\text{SiO}_2}$. All the dependences are shown in the distance ranges (a) from 0.2 to 0.7 μm and (b) from 0.7 to 2 μm . Besides that, the region of separation from 0.2 to 0.35 μm is shown in the inset to Fig. 1(a) on an enlarged scale. The minimum separation is chosen in order the characteristic frequencies contributing to the Casimir pressure be well inside the application energy range of the Dirac model. As is seen in Fig. 1, for a hotter SiO_2 plate than the environment the effects of nonequilibrium are larger than for a colder one.

In Fig. 2, the impact of graphene coating on the Casimir pressure is illustrated for (a) equilibrium and (b) nonequilibrium pressures. Thus, Fig. 2(a) shows the ratio $P_{\text{eq}}/P_{\text{eq}}^{\text{SiO}_2}$ as the function of separation by the four lines counted from bottom to top. The bottom line is computed for the chemical potential $\mu = 0$ and the energy gap $\Delta = 0.2$ eV of graphene coating, the middle line — for $\mu = 0$, $\Delta = 0.1$ eV, and the two overlapping top lines for $\mu = 0.25$ eV, $\Delta = 0.1$ and 0.2 eV. Here, P_{eq} is the Casimir pressure on a graphene-coated plate

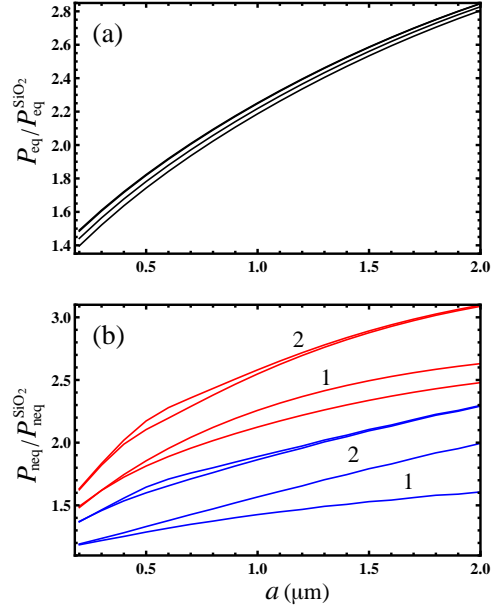


FIG. 2: The ratios of the (a) equilibrium and (b) nonequilibrium Casimir pressures for the graphene-coated SiO_2 plates to the (a) equilibrium and (b) nonequilibrium Casimir pressures for the uncoated plates are shown as the functions of separation with the following parameters of graphene coatings: (a) the four lines counted from bottom to top are computed for $\mu = 0, \Delta = 0.2$ eV; $\mu = 0, \Delta = 0.1$ eV; $\mu = 0.25$ eV, $\Delta = 0.1$ eV; $\mu = 0.25$ eV, $\Delta = 0.2$ eV and (b) the bottom and top pairs of lines labeled 1 and 2 are computed at $T = 77$ K and 500 K, respectively; for the pairs of lines 1 $\mu = 0$ and for the pairs of lines 2 $\mu = 0.25$ eV; in each pair, $\Delta = 0.2$ and 0.1 eV for the lower and upper lines, respectively.

and $P_{\text{eq}}^{\text{SiO}_2}$ on an uncoated one which is shown by the middle line in Fig. 1. It is seen that the graphene coating increases the magnitude of the equilibrium Casimir pressure and this increase is more marked for a smaller energy gap and larger chemical potential.

In Fig. 2(b), the ratio $P_{\text{neq}}/P_{\text{neq}}^{\text{SiO}_2}$ is shown as the function of separation by the two bottom pairs of lines 1 and 2 computed at $T_2 = 77$ K and two top pairs of lines 1 and 2 computed at $T_2 = 500$ K. For the pairs of lines labeled 1, the chemical potential $\mu = 0$ and for the pairs of lines labeled 2 — $\mu = 0.25$ eV. In doing so, in each pair the lower line was computed with the energy gap of graphene coating $\Delta = 0.2$ eV and the upper line — with $\Delta = 0.1$ eV. Note that the values of $P_{\text{neq}}^{\text{SiO}_2}$ for an uncoated plate are given by the bottom and top lines in Fig. 1 for $T_2 = 77$ K and $T_2 = 500$ K, respectively. As is seen in Fig. 2(b), the magnitude of nonequilibrium Casimir pressure is also increased by the graphene coating. This increase is greater for higher temperature than that of the environment and for larger chemical potential of graphene coating. Decrease of the energy gap makes an impact of graphene coating on the nonequilibrium Casimir pressure stronger.

We consider next the relative error arising in both equilibrium and nonequilibrium Casimir pressures in the configuration of two graphene-coated plates when the dielectric response of graphene coating is described in the spatially local approximation, i.e., with no regard for the spatial dispersion. In the equilibrium case, this error is given by

$$\delta P_{\text{eq}}^{\text{loc}}(a, T_E) = \frac{P_{\text{eq}}^{\text{loc}}(a, T_E) - P_{\text{eq}}(a, T_E)}{P_{\text{eq}}(a, T_E)}. \quad (22)$$

Here, in order to calculate $P_{\text{eq}}^{\text{loc}}$, the limit of $v_F k/\omega \rightarrow 0$ in the polarization tensor should be taken first. The obtained expressions are considered at the pure imaginary Matsubara frequencies $\omega = i\xi_l$ as discussed in Sec. III.

In Fig. 3, the relative error (22) in the equilibrium Casimir pressure arising when using the local approximation is shown as the function of separation by the three lines counted from bottom to top for the energy gap of graphene coatings $\Delta = 0.1, 0.2,$ and 0.3 eV, respectively, whereas the chemical potential is equal to (a) $\mu = 0$ and (b) $\mu = 0.25$ eV. As is seen in Fig. 3(a,b), the error due to using the local approximation in the dielectric response of graphene in the state of thermal equilibrium increases with increasing energy gap and decreases with increasing separation. For the graphene coating with zero chemical potential it reaches 12% at the shortest separation but becomes less than a fraction of a percent for graphene coating with $\mu = 0.25$ eV.

We are coming now to the relative error in the nonequilibrium Casimir pressure which arises from using the spatially local description of the dielectric response of graphene coating. This error is described by the quantity.

$$\delta P_{\text{neq}}^{\text{loc}}(a, T_1, T_2) = \frac{P_{\text{neq}}^{\text{loc}}(a, T_1, T_2) - P_{\text{neq}}(a, T_1, T_2)}{P_{\text{neq}}(a, T_1, T_2)}. \quad (23)$$

In Fig. 4, the computational results for $\delta P_{\text{neq}}^{\text{loc}}$ for the second plate cooled down to $T_2 = 77$ K are presented as the functions of separation by the three lines counted from bottom to top for the values of the energy gap $\Delta = 0.1, 0.2,$ and 0.3 eV, respectively, and of the chemical potential (a) $\mu = 0$ and (b) $\mu = 0.25$ eV.

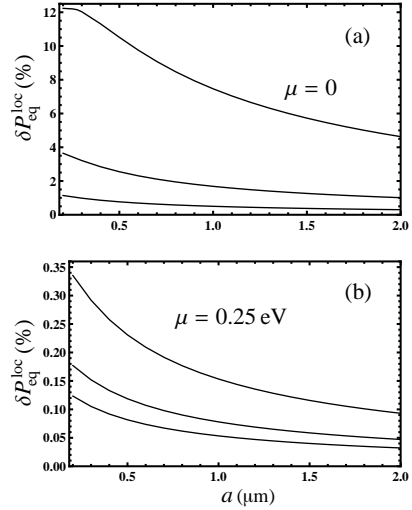


FIG. 3: The relative error in the equilibrium Casimir pressure for the graphene-coated plates arising when using the spatially local approximation in the dielectric response of graphene coatings is shown as the function of separation by the three lines counted from bottom to top for the values of the energy gap $\Delta = 0.1, 0.2,$ and 0.3 eV, respectively, and of the chemical potential (a) $\mu = 0$ and (b) $\mu = 0.25$ eV.

top for the energy gap of graphene coating $\Delta = 0.1, 0.2,$ and 0.3 eV, respectively, and the chemical potential (a) $\mu = 0$ and (b) $\mu = 0.25$ eV (recall that $T_1 = T_E = 300$ K). As is seen in Fig. 4(a,b), for the cooled graphene coating with $\mu = 0$ the error arising from using the spatially local description increases with increasing energy gap and separation within the separation range considered. Thus, for $a = 2 \mu\text{m}$ and $\Delta = 0.3$ eV it exceeds 50%. At the same time, for a graphene coating with $\mu = 0.25$ eV, this error decreases with increasing separation

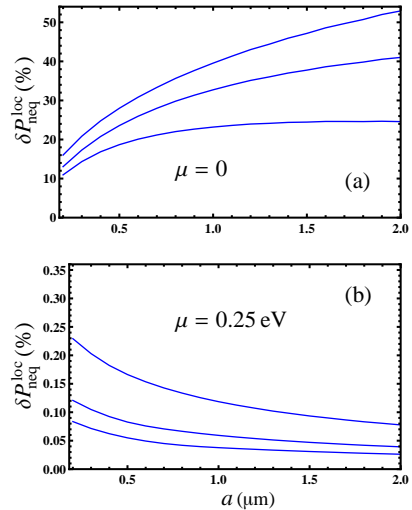


FIG. 4: The relative error in the nonequilibrium Casimir pressure for the graphene-coated plate cooled to 77 K, which arises when using the spatially local approximation in the dielectric response of graphene coatings, is shown as the function of separation by the three lines counted from bottom to top for the values of the energy gap $\Delta = 0.1, 0.2,$ and 0.3 eV, respectively, and of the chemical potential (a) $\mu = 0$ and (b) $\mu = 0.25$ eV.

and takes the values below 1% even for largest value of the energy gap considered.

The computational results for $\delta P_{\text{neq}}^{\text{loc}}$ for the heated second plate up to $T_2 = 500$ K are presented in Fig. 5 in the same form and using the same notations as in Fig. 4. From Fig. 5(a,b) it is seen that in the case of a heated plate the error of the spatially local approximation again increases with increasing energy gap but decreases with increasing separation between the plates for both values of the chemical potential considered. The maximum value of this error of 9% is reached for the graphene coating with $\mu = 0$ at $a = 0.2 \mu\text{m}$. For the doped graphene coatings with $\mu = 0.25$ eV, the error from using the spatially local approximation is again below a fraction of a percent.

Finally we consider the role of the effects of nonequilibrium in the Casimir pressure on a graphene-coated plate when the exact calculation method is used. For this purpose, we consider the ratio $P_{\text{neq}}/P_{\text{eq}}$ for different values of the energy gap and chemical potential of graphene coatings, where P_{neq} is calculated at either $T_2 = 77$ K or 500 K and P_{eq} at $T_1 = T_2 = T_E = 300$ K.

The computational results for the ratio $P_{\text{neq}}/P_{\text{eq}}$ are presented in Fig. 6 as the functions of separation by the top and bottom pairs of lines computed at $T_2 = 500$ K and 77 K, respectively, (a) for $\mu = 0$ and (b) for $\mu = 0.25$ eV. In each pair, the lower line was computed for the graphene coating with $\Delta = 0.1$ eV and the upper line — with $\Delta = 0.2$ eV using the exact formalism taking into account the spatial dispersion.

From Fig. 6(a,b) it is seen that the effects of nonequilibrium increase the magnitude of the equilibrium Casimir pressure for a heated plate and decrease it for a cooled plate. For a heated plate, the increase in the magnitude of the Casimir pressure is more pronounced for the larger energy gap. For

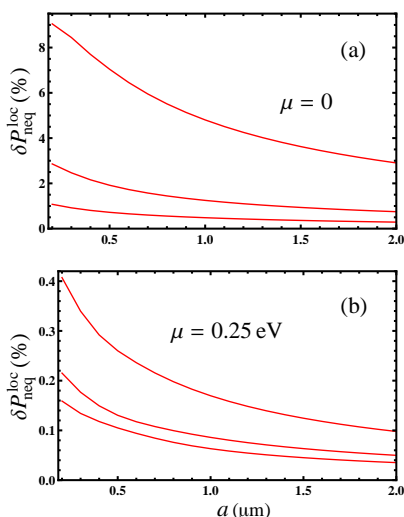


FIG. 5: The relative error in the nonequilibrium Casimir pressure for the graphene-coated plate heated to 500 K, which arises when using the spatially local approximation in the dielectric response of graphene coatings, is shown as the function of separation by the three lines counted from bottom to top for the values of the energy gap $\Delta = 0.1, 0.2,$ and 0.3 eV, respectively, and of the chemical potential (a) $\mu = 0$ and (b) $\mu = 0.25$ eV.

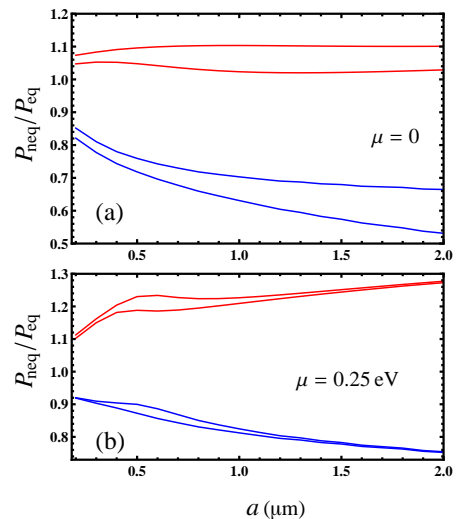


FIG. 6: The ratio of the nonequilibrium Casimir pressure for the graphene-coated SiO_2 plates computed using the exact theory to the equilibrium one is shown as the function of separation by the top and bottom pairs of lines for the plate temperatures 500 K and 77 K, respectively, and the chemical potential (a) $\mu = 0$ and (b) $\mu = 0.25$ eV. In each pair, the energy gap is equal to $\Delta = 0.1$ and 0.2 eV for the lower and upper lines, respectively.

a cooled plate, however, the decrease in the magnitude of the Casimir pressure is greater for a smaller energy gap. By comparing Figs. 6(a) and 6(b), one can conclude that the effects of nonequilibrium make the larger impact on the equilibrium pressure for the graphene coatings with $\mu = 0.25$ eV than for $\mu = 0$. It is seen also that for larger μ an impact of the energy gap on the effects of nonequilibrium becomes smaller.

V. CONCLUSIONS AND DISCUSSION

In the foregoing, we have presented the more compact and convenient in computations analytic form for the polarization tensor of graphene along the real frequency axis which can be applied to theoretical description of many diverse phenomena in graphene systems, such as the nonequilibrium Casimir and Casimir-Polder interactions, surface plasmons, reflectances of graphene and graphene-coated substrates, electrical conductivity, radiation heat transfer, etc. As an example, we calculated the nonequilibrium Casimir pressure in the configuration of two parallel graphene-coated plates one of which is either hotter or colder than the environment. It should be stressed that in the framework of the Dirac model the field theoretical formalism using the polarization tensor takes a full account of the spatial dispersion in graphene coatings which was disregarded previously. Worthy of mention also are the experiments on measuring the gradient of the equilibrium Casimir force between an Au-coated sphere and a graphene-coated plate which were found in a very good agreement with the theoretical predictions using the formalism of the polarization tensor [79, 84–86].

Using the reflection coefficients on the graphene-coated sil-

ica glass plates expressed in terms of the frequency-dependent dielectric permittivity of the plate material and the polarization tensor, we performed numerical computations of the nonequilibrium Casimir pressure on a hotter and colder plates than the environment. The cases of both equilibrium and nonequilibrium Casimir pressures in the configuration of uncoated silica glass plates were also considered for comparison purposes. It was shown that graphene coating increases the magnitude of the nonequilibrium Casimir pressure. This increase is greater for a higher temperature T , larger chemical potential μ and smaller energy gap Δ of graphene coatings.

The special attention was paid to the relative error in both the equilibrium and nonequilibrium Casimir pressures computed in the spatially local approximation which disregards the effects of spatial dispersion in the dielectric response of graphene coatings. According to our results, in the equilibrium Casimir pressure this error increases with increasing Δ and decreases with increasing μ and separation a between the plates. For a cooled graphene-coated plate with $\mu = 0$, the relative error in the nonequilibrium Casimir pressure increases up to 50% with increasing Δ and a . However, for a graphene coating with $\mu = 0.25$ eV, this error decreases with increasing a and remains below 1% even for the largest value of Δ considered. Different situation was demonstrated for a nonequilibrium Casimir pressure on a heated graphene-coated plate. Here, the relative error due to the use of the spatially local approximation increases with increasing Δ but decreases with increasing μ and a . The maximum error of about 9% is reached

for $\mu = 0$ at the shortest separation considered.

Finally, we have found the contribution of the effects of nonequilibrium to the total pressure by computing the ratio of the nonequilibrium to equilibrium Casimir pressures. It was shown that the effects of nonequilibrium increase the magnitude of the equilibrium Casimir pressure for a hotter graphene-coated plate than the environment and decrease it for a colder plate. For a hotter plate, the increase is larger for larger Δ of the graphene coating but for a colder plate the decrease in the pressure magnitude is larger for a smaller Δ . The impact of the value of Δ decreases with increasing μ .

By and large, the obtained results demonstrate that the physical phenomena determined by the electromagnetic fluctuations in graphene systems should be described with taken into account spatial dispersion in the dielectric response of graphene, its temperature, chemical potential, and the energy gap. A comprehensive description of this kind is given in the framework of thermal quantum field theory using the formalism of the polarization tensor. This formalism can be used in numerous applications of graphene in both fundamental physics and nanotechnology.

Acknowledgments

The work of G.L.K. and V.M.M. was supported by the State assignment for basic research (project FSEG-2023-0016).

-
- [1] K. S. Novoselov, A. K. Geim, S. V. Morozov, D. Jiang, Y. Zhang, S. V. Dubonov, I. V. Grigorieva, and A. A. Firsov, *Electric Field Effect in Atomically Thin Carbon Films*, *Science* **306**, 666 (2004).
- [2] A. K. Geim and K. S. Novoselov, *The rise of graphene*, *Nature Materials* **6**, 183 (2007).
- [3] A. H. Castro Neto, F. Guinea, N. M. R. Peres, K. S. Novoselov, and A. K. Geim, *The electronic properties of graphene*, *Rev. Mod. Phys.* **81**, 109 (2009).
- [4] M. I. Katsnelson, *The Physics of Graphene* (Cambridge University Press, Cambridge, 2020).
- [5] M. I. Katsnelson, K. S. Novoselov, and A. K. Geim, *Chiral tunnelling and the Klein Paradox in graphene*, *Nat. Phys.* **2**, 620 (2006).
- [6] M. O. Goerbig, *Electronic properties of graphene in a strong magnetic field*, *Rev. Mod. Phys.* **83**, 1193 (2011).
- [7] D. Allor, T. D. Cohen, and D. A. McGady, *Schwinger mechanism and graphene*, *Phys. Rev. D* **78**, 096009 (2008).
- [8] C. G. Beneventano, P. Giacconi, E. M. Santangelo, and R. Soldati, *Planar QED at finite temperature and density: Hall conductivity, Berry's phases and minimal conductivity of graphene*, *J. Phys. A* **42**, 275401 (2009).
- [9] G. L. Klimchitskaya and V. M. Mostepanenko, *Creation of quasiparticles in graphene by a time-dependent electric field*, *Phys. Rev. D* **87**, 125011 (2013).
- [10] I. Akal, R. Egger, C. Müller, and S. Villalba-Chávez, *Low-dimensional approach to pair production in an oscillating electric field: Application to bandgap graphene layers*, *Phys. Rev. D* **93**, 116006 (2016).
- [11] I. Akal, R. Egger, C. Müller, and S. Villalba-Chávez, *Simulating dynamically assisted production of Dirac pairs in gapped graphene monolayers*, *Phys. Rev. D* **99**, 016025 (2019).
- [12] A. Golub, R. Egger, C. Müller, and S. Villalba-Chávez, *Dimensionality-Driven Photoproduction of Massive Dirac Pairs near Threshold in Gapped Graphene Monolayers*, *Phys. Rev. Lett.* **124**, 110403 (2020).
- [13] R. D. Pisarski, *Chiral-symmetry breaking in three-dimensional electrostatics*, *Phys. Rev. D* **29**, 2423(R) (1984).
- [14] T. W. Appelquist, M. Bowick, D. Karabali, and L. C. R. Wijewardhana, *Spontaneous chiral-symmetry breaking in three-dimensional QED*, *Phys. Rev. D* **33**, 3704 (1986).
- [15] C. J. Burden, J. Praszifka, and C. D. Roberts, *Photon polarization tensor and gauge dependence in three-dimensional quantum electrostatics*, *Phys. Rev. D* **46**, 2695 (1992).
- [16] B. M. Pimentel, A. T. Suzuki, and J. L. Tomazelli, *Vacuum polarization tensor in three-dimensional quantum electrodynamics*, *Int. J. Mod. Phys. A* **7**, 5307 (1992).
- [17] N. Dorey and N. E. Mavromatos, *QED-3 and two-dimensional superconductivity without parity violation*, *Nucl. Phys. B* **386**, 614 (1992).
- [18] E. V. Gorbar, V. P. Gusynin, V. A. Miransky, and I. A. Shovkovy, *Magnetic field driven metal-insulator phase transition in planar systems*, *Phys. Rev. B* **66**, 045108 (2002).
- [19] V. P. Gusynin and S. G. Sharapov, *Transport of Dirac quasiparticles in graphene: Hall and optical conductivities*, *Phys. Rev. B* **73**, 245411 (2006).
- [20] P. K. Pyatkovsky, *Dynamical polarization, screening, and plasmons in gapped graphene*, *J. Phys.: Condens. Matter* **21**,

- 025506 (2009).
- [21] W. Li and G.-Z. Liu, Dynamical chiral symmetry breaking in QED-3 at finite density and impurity potential, *Phys. Rev. D* **81**, 045006 (2010).
- [22] M. Bordag, I. V. Fialkovsky, D. M. Gitman, and D. V. Vassilevich, Casimir interaction between a perfect conductor and graphene described by the Dirac model, *Phys. Rev. B* **80**, 245406 (2009).
- [23] I. V. Fialkovsky, V. N. Marachevsky, and D. V. Vassilevich, Finite-temperature Casimir effect for graphene, *Phys. Rev. B* **84**, 035446 (2011).
- [24] M. Bordag, G. L. Klimchitskaya, V. M. Mostepanenko, and V. M. Petrov, Quantum field theoretical description for the reflectivity of graphene, *Phys. Rev. D* **91**, 045037 (2015); **93**, 089907(E) (2016).
- [25] M. Bordag, I. Fialkovskiy, and D. Vassilevich, Enhanced Casimir effect for doped graphene, *Phys. Rev. B* **93**, 075414 (2016); **95**, 119905(E) (2017).
- [26] M. Bordag, G. L. Klimchitskaya, and V. M. Mostepanenko, Convergence of the polarization tensor in spacetime of three dimensions, *Phys. Rev. D* **109**, 125014 (2024).
- [27] M. Bordag, G. L. Klimchitskaya, and V. M. Mostepanenko, Thermal Casimir effect in the interaction of graphene with dielectrics and metals, *Phys. Rev. B* **86**, 165429 (2012).
- [28] M. Chaichian, G. L. Klimchitskaya, V. M. Mostepanenko, and A. Tureanu, Thermal Casimir-Polder interaction of different atoms with graphene, *Phys. Rev. A* **86**, 012515 (2012).
- [29] G. L. Klimchitskaya and V. M. Mostepanenko, Van der Waals and Casimir interactions between two graphene sheets, *Phys. Rev. B* **87**, 075439 (2013).
- [30] B. Arora, H. Kaur, and B. K. Sahoo, C_3 coefficients for the alkali atoms interacting with a graphene and carbon nanotube, *J. Phys. B* **47**, 155002 (2014).
- [31] K. Kaur, J. Kaur, B. Arora, and B. K. Sahoo, Emending thermal dispersion interaction of Li, Na, K and Rb alkali-metal atoms with graphene in the Dirac model, *Phys. Rev. B* **90**, 245405 (2014).
- [32] G. L. Klimchitskaya and V. M. Mostepanenko, Observability of thermal effects in the Casimir interaction from graphene-coated substrates, *Phys. Rev. A* **89**, 052512 (2014).
- [33] G. L. Klimchitskaya, V. M. Mostepanenko, and Bo E. Sernelius, Two approaches for describing the Casimir interaction with graphene: density-density correlation function versus polarization tensor, *Phys. Rev. B* **89**, 125407 (2014).
- [34] G. L. Klimchitskaya and V. M. Mostepanenko, Origin of large thermal effect in the Casimir interaction between two graphene sheets, *Phys. Rev. B* **91**, 174501 (2015).
- [35] G. Bimonte, G. L. Klimchitskaya, and V. M. Mostepanenko, How to observe the giant thermal effect in the Casimir force for graphene systems, *Phys. Rev. A* **96**, 012517 (2017).
- [36] G. Bimonte, G. L. Klimchitskaya, and V. M. Mostepanenko, Thermal effect in the Casimir force for graphene and graphene-coated substrates: Impact of nonzero mass gap and chemical potential, *Phys. Rev. B* **96**, 115430 (2017).
- [37] C. Henkel, G. L. Klimchitskaya, and V. M. Mostepanenko, Influence of chemical potential on the Casimir-Polder interaction between an atom and gapped graphene or graphene-coated substrate, *Phys. Rev. A* **97**, 032504 (2018).
- [38] G. L. Klimchitskaya and V. M. Mostepanenko, Low-temperature behavior of the Casimir-Polder free energy and entropy for an atom interacting with graphene, *Phys. Rev. A* **98**, 032506 (2018).
- [39] G. L. Klimchitskaya and V. M. Mostepanenko, The Nernst heat theorem for an atom interacting with graphene: Dirac model with nonzero energy gap and chemical potential, *Phys. Rev. D* **101**, 116003 (2020).
- [40] N. Khusnutdinov and N. Emelianova, Low-temperature expansion of the Casimir-Polder free energy for an atom interacting with a conducting plane, *Int. J. Mod. Phys. A* **34**, 1950008 (2019).
- [41] G. L. Klimchitskaya and V. M. Mostepanenko, Quantum field theoretical description of the Casimir effect between two real graphene sheets and thermodynamics, *Phys. Rev. D* **102**, 016006 (2020).
- [42] G. L. Klimchitskaya and V. M. Mostepanenko, Quantum field theoretical framework for the electromagnetic response of graphene and dispersion relations with implications to the Casimir effect, *Phys. Rev. D* **107**, 105007 (2023).
- [43] G. L. Klimchitskaya and V. M. Mostepanenko, Reflectivity properties of graphene with nonzero mass-gap parameter, *Phys. Rev. A* **93**, 052106 (2016).
- [44] G. L. Klimchitskaya and V. M. Mostepanenko, Optical properties of dielectric plates coated with gapped graphene, *Phys. Rev. B* **95**, 035425 (2017).
- [45] G. L. Klimchitskaya, V. M. Mostepanenko, and V. M. Petrov, Impact of chemical potential on the reflectance of graphene in the infrared and microwave domains, *Phys. Rev. A* **98**, 023809 (2018).
- [46] G. L. Klimchitskaya and V. M. Mostepanenko, Conductivity of pure graphene: Theoretical approach using the polarization tensor, *Phys. Rev. B* **93**, 245419 (2016).
- [47] G. L. Klimchitskaya and V. M. Mostepanenko, Quantum electrodynamic approach to the conductivity of gapped graphene, *Phys. Rev. B* **94**, 195405 (2016).
- [48] G. L. Klimchitskaya, V. M. Mostepanenko, and V. M. Petrov, Conductivity of graphene in the framework of Dirac model: Interplay between nonzero mass gap and chemical potential, *Phys. Rev. B* **96**, 235432 (2017).
- [49] G. L. Klimchitskaya and V. M. Mostepanenko, Kramers-Kronig relations and causality conditions for graphene in the framework of the Dirac model, *Phys. Rev. D* **97**, 085001 (2018).
- [50] M. Bordag and I. G. Pirozhenko, Surface plasmons for doped graphene, *Phys. Rev. D* **91**, 085038 (2015).
- [51] M. Bordag and I. G. Pirozhenko, QED and surface plasmons on graphene, *Int. J. Mod. Phys. A* **31**, 1641027 (2016).
- [52] M. Bordag and I. G. Pirozhenko, Surface plasmons on graphene at finite T , *Int. J. Mod. Phys. B* **30**, 1650120 (2016).
- [53] E. M. Lifshitz, The theory of molecular attractive forces between solids, *Zh. Eksp. Teor. Fiz.* **29**, 94 (1955) [*Sov. Phys. JETP* **2**, 73 (1956)].
- [54] I. E. Dzyaloshinskii, E. M. Lifshitz, and L. P. Pitaevskii, General theory of van der Waals forces, *Usp. Fiz. Nauk* **73**, 381 (1961) [*Sov. Phys. Usp.* **4**, 153 (1961)].
- [55] E. M. Lifshitz and L. P. Pitaevskii, *Statistical Physics, Part II* (Pergamon, Oxford, 1980).
- [56] I. A. Dorofeyev, The force of attraction between two solids with different temperatures, *J. Phys. A: Math. Gen.* **31**, 4369 (1998).
- [57] G. Bimonte, A Theory of Electromagnetic Fluctuations for Metallic Surfaces and van der Waals Interactions between Metallic Bodies, *Phys. Rev. Lett.* **96**, 160401 (2006).
- [58] M. Antezza, L. P. Pitaevskii, S. Stringari, and V. B. Svetovoy, Casimir-Lifshitz Force Out of Thermal Equilibrium and Asymptotic Nonadditivity, *Phys. Rev. Lett.* **97**, 223203 (2006).
- [59] M. Antezza, L. P. Pitaevskii, S. Stringari, and V. B. Svetovoy, Casimir-Lifshitz force out of thermal equilibrium, *Phys. Rev. A* **77**, 022901 (2008).
- [60] G. Bimonte, T. Emig, M. Krüger, and M. Kardar, Dilution and resonance-enhanced repulsion in nonequilibrium fluctua-

- tion forces, *Phys. Rev. A* **84**, 042503 (2011).
- [61] C. Henkel, K. Joulain, J.-P. Mulet, and J.-J. Greffet, Radiation forces on small particles in thermal near fields, *J. Opt. A: Pure Appl. Opt.* **4**, S109 (2002).
- [62] M. Antezza, L. P. Pitaevskii, and S. Stringari, New Asymptotic Behavior of the Surface-Atom Force out of Thermal Equilibrium, *Phys. Rev. Lett.* **95**, 113202 (2005).
- [63] G. Bimonte, Scattering approach to Casimir forces and radiative heat transfer for nanostructured surfaces out of thermal equilibrium, *Phys. Rev. A* **80**, 042102 (2009).
- [64] R. Messina and M. Antezza, Scattering-matrix approach to Casimir-Lifshitz force and heat transfer out of thermal equilibrium between arbitrary bodies, *Phys. Rev. A* **84**, 042102 (2011).
- [65] R. Messina and M. Antezza, Casimir-Lifshitz force out of thermal equilibrium and heat transfer between arbitrary bodies, *EPL* **95**, 61002 (2011).
- [66] M. Krüger, T. Emig, and M. Kardar, Nonequilibrium Electromagnetic Fluctuations: Heat Transfer and Interactions, *Phys. Rev. Lett.* **106**, 210404 (2011).
- [67] M. Krüger, T. Emig, G. Bimonte, and M. Kardar, Nonequilibrium Casimir forces: Spheres and sphere-plate, *EPL* **95**, 21002 (2011).
- [68] M. Krüger, G. Bimonte, T. Emig, and M. Kardar, Trace formulas for nonequilibrium Casimir interactions, heat radiation, and heat transfer for arbitrary bodies, *Phys. Rev. B* **86**, 115423 (2012).
- [69] R. Messina and M. Antezza, Three-body radiative heat transfer and Casimir-Lifshitz force out of thermal equilibrium for arbitrary bodies, *Phys. Rev. A* **89**, 052104 (2014).
- [70] A. Noto, R. Messina, B. Guizal, and M. Antezza, Casimir-Lifshitz force out of thermal equilibrium between dielectric gratings, *Phys. Rev. A* **90**, 022120 (2014).
- [71] G.-L. Ingold, G. L. Klimchitskaya, and V. M. Mostepanenko, Nonequilibrium effects in the Casimir force between two similar metallic plates kept at different temperatures, *Phys. Rev. A* **101**, 032506 (2020).
- [72] G. L. Klimchitskaya and V. M. Mostepanenko, Casimir-Polder Interaction of an Atom with a Cavity Wall Made of Phase-Change Material out of Thermal Equilibrium, *Atoms* **9**, 4 (2021).
- [73] G. L. Klimchitskaya, V. M. Mostepanenko, and O. Yu. Tsybin, Casimir-Polder attraction and repulsion between nanoparticles and graphene in out-of-thermal-equilibrium conditions, *Phys. Rev. B* **105**, 195430 (2022); **109**, 079901(E) (2024).
- [74] G. L. Klimchitskaya, C. C. Korikov, V. M. Mostepanenko, and O. Yu. Tsybin, Impact of Mass-Gap on the Dispersion Interaction of Nanoparticles with Graphene out of Thermal Equilibrium, *Appl. Sci.* **13**, 7511 (2023).
- [75] G. L. Klimchitskaya, C. C. Korikov, V. M. Mostepanenko, and O. Yu. Tsybin, Nonequilibrium Casimir-Polder Interaction Between Nanoparticles and Substrates Coated with Gapped Graphene, *Symmetry* **15**, 1580 (2023); **16**, 274(E) (2024).
- [76] G. L. Klimchitskaya, C. C. Korikov, and V. M. Mostepanenko, Nonequilibrium Casimir-Polder Force between Nanoparticles and Graphene-Coated Silica Plate: Combined Effect of the Chemical Potential and Mass Gap, *Symmetry* **16**, 320 (2024).
- [77] Y. Jeyar, K. Austray, M. Luo, B. Guizal, H. B. Chan, and M. Antezza, Casimir-Lifshitz force between graphene-based structures out of thermal equilibrium, *Phys. Rev. B* **108**, 115412 (2023).
- [78] D. Polder and M. Van Hove, Theory of radiative heat transfer between closely spaced bodies, *Phys. Rev. B* **4**, 3303 (1971).
- [79] G. L. Klimchitskaya, U. Mohideen, and V. M. Mostepanenko, Theory of the Casimir interaction for graphene-coated substrates using the polarization tensor and comparison with experiment, *Phys. Rev. B* **89**, 115419 (2014).
- [80] V. P. Gusynin, S. G. Sharapov, and J. P. Carbotte, On the universal ac optical background in graphene, *New J. Phys.* **11**, 095013 (2009).
- [81] S. A. Jafari, Nonlinear optical response in gapped graphene, *J. Phys.: Condens. Matter* **24**, 205802 (2012).
- [82] *Handbook of Optical Constants of Solids*, edited by E. D. Palik (Academic, New York, 1985).
- [83] M. Bordag, G. L. Klimchitskaya, U. Mohideen, and V. M. Mostepanenko, *Advances in the Casimir Effect* (Oxford University Press, Oxford, 2015).
- [84] A. A. Banishev, H. Wen, J. Xu, R. K. Kawakami, G. L. Klimchitskaya, V. M. Mostepanenko, and U. Mohideen, Measuring of the Casimir force gradient from graphene on a SiO₂ substrate, *Phys. Rev. B* **87**, 205433 (2013).
- [85] M. Liu, Y. Zhang, G. L. Klimchitskaya, V. M. Mostepanenko, and U. Mohideen, Demonstration of Unusual Thermal Effect in the Casimir Force for Graphene, *Phys. Rev. Lett.* **126**, 206802 (2021).
- [86] M. Liu, Y. Zhang, G. L. Klimchitskaya, V. M. Mostepanenko, and U. Mohideen, Experimental and theoretical investigation of the thermal effect in the Casimir interaction from graphene, *Phys. Rev. B* **104**, 085436 (2021).